J|A|C|S
ARTICLES
Published on Web 05/31/2002

The Mechanism of Cis−Trans Isomerization of Prolyl Peptides by Cyclophilin

Sun Hur and Thomas C. Bruice*

Contribution from the Department of Chemistry and Biochemistry, University of California, Santa Barbara, California 93106

Received February 13, 2002. Revised Manuscript Received April 19, 2002

Abstract: The mechanism of cis−trans isomerization of prolyl peptides catalyzed by cyclophilin (CyP) was studied computationally via molecular dynamics (MD) simulations of the transition state (TS) and the cis and trans forms of the ground state (GS), when bound to CyP and when free in aqueous solution. The MD simulations include four enzyme-bound species of tetrapeptide (Suc-Ala-X**C(═O)-N**Pro-Phe-*p*NA; X = Gly, Trp, Ala, and Leu). In water, the prolyl amide bond is favorably planar with the presence of conformers exhibiting ±20° twist of the C−N dihedral. In the active site a hydrogen bond between the *cis*-prolyl amide carbonyl O and the backbone amide N−H of Asn102 retains the 20° twist of the C−N dihedral. The TS structure is characterized by a 90° twist of the amide C−N bond and a more favorable interaction with Asn102 due to the shorter distance between Asn102(HN) and the amide carbonyl O. The conformational change of cis → TS also involves pyramidalization of the amide N, which results in the formation of a hydrogen bond between the amide N and the guanidino group of Arg55. Both Asn102 and Arg55 are held in the same position in CyP·cis-isomer as in CyP·TS. In the ligand-free CyP the Arg55 guanidino group is highly disorganized and Asn102 is displaced 1 Å from the position in the ligand-bound CyP. Thus, the organization of Arg55 and Asn102 occurs upon substrate binding. The geometrical complimentarity of the organized enzyme structure to the TS structure is a result of preferential binding of the proline N and the amide carbonyl of the TS compared to that of GS. However, the N-terminal part (Suc-Ala) becomes repositioned in the TS such that two hydrogen bonds disappear, one hydrogen bond appears and two other hydrogen bonds becomes weaker on the conversion of CyP·*cis* to CyP·TS. During this conversion, total hydrophobic contact between enzyme and the peptide is preserved. Thus, the interaction energies of GS and TS with enzyme are, as a whole, much alike. This does not support the contention that TS is bound more tightly than GS by $K_m/K_{TS} = 10^6$ in the cis → trans reaction. Repositioning of the N-terminal part of the peptide on CyP·TS formation becomes more pronounced when the substrate X residue is changed from Gly < Trp < Ala < Leu. We propose that the larger turning of the N-terminus is responsible for the larger value of the experimentally observed $\Delta S^{\ddagger}$ and $\Delta H^{\ddagger}$, which sum up to little change in $\Delta G^{\ddagger}$. The positioning of the Arg55 and the degree of 20° twist of the amide C−N bond are considered as criteria for Near Attack Conformers (NACs) in cis−trans isomerization. NACs account for ∼30% of the total GS populations of the cis-isomer. Similar NAC populations were observed with four different substrates. This is consistent with the insensitivity of enzymatic activity to the nature of the X residue. Also, the NAC population in CyP·*trans*-AAPF was comparable to that in CyP·*cis*-AAPF, in accord with similar experimentally measured rates of the cis → trans and trans → cis reaction in CyP. These NACs, found in CyP·*cis* and CyP·*trans*, resemble only one of the four possible TS configurations in the water reaction. The identity of this TS structure (syn/exo) is in accord with experimentally determined KIE values in the enzymatic reaction. However, the geometry of the active site was also complementary to another TS structure (anti/exo) that was not detected in the active site by the same KIE measurements, implying that the geometrical fitness of the TS cannot be a single determining factor for enzymatic reactions.

Introduction

Preferential binding of the transition state (TS), as compared to the substrate ground state (GS), is the most often used explanation for the efficiency of enzymatic catalysis.[1] Theoretical arguments for the tenet that TS stabilization drives enzyme catalysis are based upon Scheme 1. In this model, K_{TS} is the ratio of nonenzymatic reaction rate over enzymatic reaction rate: $K_{TS} = k_{non}(K_m/k_{cat})$. The equilibrium constant for dis-

Scheme 1

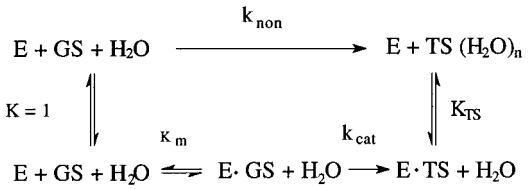

* To whom correspondences should be addressed. E-mail: tcbruice@bioorganic.ucsb.edu.

(1) Pauling, L. *Chem. Eng. News* **1946**, *24*, 1375−1377.

Scheme 2

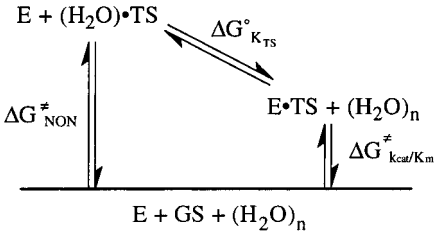

Scheme 3

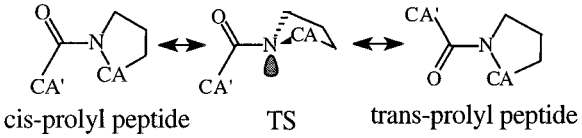

sociation of E·TS in water is generally taken as K_{TS}.[2] Observed from a different standpoint, Scheme 1 becomes Scheme 2 and $\Delta G^{\circ}_{KTS} = \Delta G^{\ddagger}_{NON} - \Delta G^{\ddagger}_{kcat}/K_m$.[3] Thus, ΔG°_{KTS} is nothing more than a measure of the difference in free energies of activation for the enzymatic and nonenzymatic reaction and this free energy difference reflects all features of the enzymatic and nonenzymatic reactions, including the binding energy difference between E·GS and E·TS.

We have initiated investigations of the dynamic structures of enzyme·ground state (E·GS) and E·TS in order to compare electrostatic and hydrophobic interactions of enzyme with GS and TS. Our interest is in answering the following questions: Is "TS-binding" a tenet of an enzyme activity, or a contributing factor? Are there enzymatic reactions in which TS binding is much less than GS binding? It has been observed for a number of enzymes[3] that K_{TS} does not reflect the binding affinity of TS. As one example, the Claisen rearrangement of chorismate into prephenate catalyzed by *E. coli* chorismate mutase has been of particular interest because this reaction is an intramolecular rearrangement without a covalent bonding interaction with enzyme and the enzymatic reaction resembles that in water. These features enable a direct interpretation of the thermodynamic cycle in Scheme 1 and thus provide a good opportunity to test the "TS-binding" tenet. We have found that in the *E. coli* mutase reaction that the TS is no more tightly bound than GS although K_m/K_{TS} is evaluated to be 10^6.[4] Instead, the chorismate mutase transforms the substrate into a conformer that closely resembles the TS geometry (Near Attack Conformer; NAC) upon its binding in the active site. Determination of the proficiency of enzymes in forming NAC's and comparison of interactions of an enzyme with NAC and TS can be performed by molecular dynamics (MD) simulation.

In the present study, we examined the cis−trans isomerization of prolyl peptides catalyzed by cyclophilin (CyP) (Scheme 3). The reaction resembles the chorismate mutase reaction insofar that both are intramolecular rearrangements without covalent interaction with the enzyme. In the CyP reaction the TS involves a twisted-amide similar to that in the noncatalyzed reaction in water. Here, we report 10 molecular dynamics (MD) simulations of CyP complexed with 4 cis's, 1 trans, and 4 TS's of succinyl-Ala-X**C(=O)-N**Pro-Phe-*p*-nitroanilide (Suc-AXPF-*p*NA) where X = Gly, Trp, Ala, and Leu. These results were compared with

Chart 1

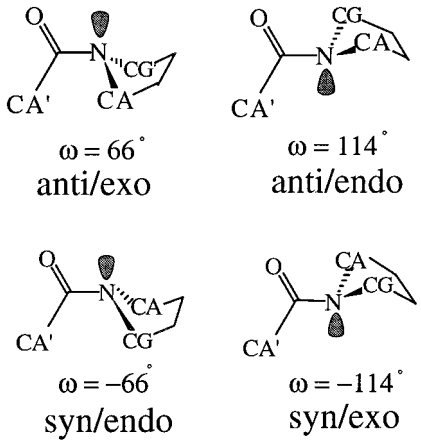

the MD simulation of ligand-free CyP and 2 MD simulations of unbound substrates (cis and trans forms of Suc-AGPF-*p*NA) in water.

Background

A peptide bond has a high energy barrier of rotation (15−20 kcal/mol). The reason for this high barrier is currently under debate but the resonance stabilization of planar cis/trans ground states significantly contributes.[5,6] Four different TS structures can be envisioned depending on the direction of rotation of C=O (anti: clockwise rotation with respect to the C−N bond from the view of *p*NA vs syn: counterclockwise) and the lone pair orientation of the amide N with respect to CA, CG, and C (exo vs endo) (Chart 1).[7] The relative stabilities of these TS conformers depend on several factors such as solvent polarity.[6,8] Due to the steric conflicts between adjacent α-carbon substituents, the cis-isomer is ∼2.6 kcal/mol less stable than the trans-isomer of a normal secondary amide.[9] The relative stability of trans-isomer compared to cis-isomer becomes less significant in a prolyl peptide because the five-membered pyrrolidine ring reduces the steric conflicts in the cis-isomer.[9] This results in the existence of ∼10% of *cis*-prolyl peptide in water.[10] However, due to the high energy barrier associated with cis−trans isomerization, the coexistence of two isomers is not physiologically meaningful unless the interconversion occurs on a rapid time scale. Indeed, the rate of cis−trans isomerization of prolyl peptides has been shown to play an important role in protein folding and cellular signaling.[11]

CyP, FKBP, and parvulin are currently known enzymes that catalyze the cis−trans isomerization of prolyl peptide bonds.[12] CyP and FKBP are believed to employ a "twisted amide" mechanism as in water (Scheme 3).[13] According to this mechanism, the amide group is distorted by noncovalent

(2) Wolfenden, R.; Snider, M. J. *Acc. Chem. Res.* **2001**, *34*, 938−945.
(3) Bruice, T. C. *Acc. Chem. Res.* **2002**, *35*, 139−148.
(4) Hur, S.; Bruice, T. C. *Proc. Natl. Acad. Sci. U.S.A.* **2002**, *99*, 1176−1181.
(5) Lauvergnant, D.; Hiberty, P. *J. Am. Chem. Soc.* **1997**, *119*, 9478−9482.
(6) Wiberg, K. B.; Rablen, P. R.; Rush, D. J.; Keith, T. A. *J. Am. Chem. Soc.* **1995**, *117*, 4261−4270.
(7) The nomenclature of the four conformers of the prolyl amide TS has not been used in a consistent manner in previous literature. In this paper, we follow the same nomenclature as in ref 14.
(8) Duffy, E. M.; Severance, D. L.; Jorgensen, W. L. *J. Am. Chem. Soc.* **1992**, *114*, 7535−7542.
(9) Ramachandran, G. N.; Sasisekharan, V. *Adv. Protein Chem.* **1968**, *23*, 283−437.
(10) Brandts, J. F.; Halvorson, H. R.; Bennan, M. *Biochemistry* **1975**, *14*, 4953−4963.
(11) Schreiber, S. L.; Albers, M. W.; Brown, E. J. *Acc. Chem. Res.* **1993**, *26*, 412−420.
(12) Fischer, G. *Chem. Soc. Rev.* **2000**, *29*, 119−127.
(13) Stein, R. L. *Adv. Protein Chem.* **1993**, *44*, 1−24.

interactions with the enzyme rather than the carbonyl C being attacked by a nucleophile, forming a covalent intermediate with the enzyme. FKBP catalyzes the reaction by $\sim 10^4$-fold compared to the water reaction and it has been concluded by computational studies that TS stabilization is an important factor in the catalysis.[14,15] However, CyP catalysis has many features different from FKBP and the mechanism has not been studied at the molecular level. The reaction is accelerated by $\sim 10^6$-fold and the barrier is mostly comprised of entropy as opposed to the larger enthalpy barrier in FKBP-catalyzed reaction.[13] CyP catalysis does not depend on the identity of the preceding residue X (in X**C(═O)-N**Pro bond rotation) but FKBP does. The Eyring plot exhibits curved dependency on inverse temperature in CyP whereas it is linear in FKBP.[13] Besides these thermodynamic/kinetic data, the residues comprising the active sites are also quite different, which is reflected in inhibitor bindings. Cyclosporin inhibits the isomerization activity of cyclophilin and FK506 does so for FKBP, but no cross inhibition was observed for both inhibitors.[16−18]

Method

Suc-Ala-X**C(═O)-N**Pro-Phe-*p*NA (X = Gly, Trp, Ala, Leu) peptides were chosen as substrates in order to take advantage of the wealth of kinetic/thermodynamic experimental data available.[13] The force fields and atomic charges for the cis and trans forms of the substrate peptide were directly employed from standard CHARMM27 parameters. The TS structure was modeled according to the gas-phase syn/exo geometry of Gly-Pro optimized at the HF/3-21G level of theory (Chart 1). This computational level is the same as used in CHARMM27 parameters for proline peptide.[19] The obtained TS structure from this ab initio calculation involves a 90° twisted amide bond. This TS geometry is appropriate for modeling the TS in the active site because NMR studies[20] show that the cis → trans and trans → cis reaction rates are similar in the CyP active site, implying that the TS of the CyP reaction is about at the middle of the reaction coordinate between the cis and trans geometries as found by ab initio calculations in the gas phase. According to the ab initio TS geometry, the bond lengths X(C)−Pro(N) and X(C)−X(O) of TS were modified (X(C)−Pro(N) = 1.43 Å, X(C)−X(O) = 1.21 Å) and all six of the angles involving the amide bond X(C)−Pro(N) were constrained by using a force constant of 500 kcal/mol/Å^2. Improper torsion at the Pro(N) was removed and ω(Pro) was fixed at 114° for the TS by using a force constant of 5000 kcal/mol. The same atomic charges were used for the TS as in the cis- or trans-isomer. Recent computational studies show that previously believed charge transfer from the amide N to the carbonyl O in the planar ground state is not correct, due to the compensating behavior of π and σ bond electrons in both N and O.[21] Using the same charges for the GS (cis- and trans-isomer) and the TS has also been adopted by Karplus et al. in the calculation of the reaction coordinate of cis-isomer → trans-isomer.[14]

Due to the large difference in the conformation of the cis- and trans-isomers, separate enzyme crystal structures were chosen for the initial coordinates for the MD simulations. For CyP•*cis*, the crystal structure complexed with cis-peptide (PDB code: 1RMH[22]) was used. For CyP•*trans*, the crystal structure with trans-peptide (PDB code: 1AWQ[23]) was used. For CyP•TS, 1RMH was used because the geometry of the crystallized substrate of 1RMH is closer to the TS than that of 1AWQ. Each type of substrate was modeled into the active site by adding and removing the side chain of X. When adding a large side chain to X, steric hindrance was minimized by rotating the side chain or other contacting residues. After completion of docking, the CyP•ligand complex with crystallographic water was energy-minimized by 200 steps of Steepest Descent (SD) method followed by 200 steps of Adopted Basis Newton−Raphson method (ABNR).[24]

The program CHARMM (version 25b2) was used for all simulations. The all-hydrogen potential function was used for all protein atoms[19] and a TIP3 water model was used for the solvent.[25] Stochastic boundary conditions were used to reduce the computational burden.[26] The system was separated into a reaction region (r < 23 Å from P3(O) of substrate), a buffer region (23 < r < 25 Å), and a reservoir region (r > 25 Å). All protein atoms in the reservoir region were fixed with harmonic constraint and all water molecules in the reservoir were deleted. A sphere of water 25 Å in radius solvates CyP except for residues which were farther than the nonbonded interaction cutoff distance (12 Å) apart from any atom of the substrate. It has been reported that binding of substrates does not significantly affect the crystal structure of the enzyme.[23] Thus, dynamics of such remote residues are not likely to propagate into the active site. The final system for all simulations consisted of 158 protein residues, 6 substrate residues, and $\sim 1370 \pm 10$ water molecules. Inside the reaction region, atoms were propagated by molecular dynamics whereas atoms in the buffer region were propagated by Langevin dynamics. Atoms inside the buffer region were restrained by a harmonic restoring force with force constants derived from the temperature factors in the crystal structure.[26] Water molecules were confined to the active site region by a deformable boundary.[27] The friction constant in the Langevin dynamics was 250 ps^{-1} for the protein atoms and 62 ps^{-1} for the water molecules.[26] During each simulation, all bonds with hydrogen atoms were fixed by the SHAKE algorithm.[19] A 1-fs time step was used for integrating the equations of motion. The system was energy minimized by 200 steps of SD followed by 200 steps of ABNR before equilibration for 100 ps at 300 K. This procedure was followed by 600−700 ps of production dynamics. Eight simulations were performed on the CyP•(*cis*-AXPF) and CyP•(TS-AXPF), where X = G, W, A, and L. For the trans-isomer, only the CyP•(*trans*-AAPF) simulation was performed due to the lack of experimental data pertaining to the trans → cis reaction of other peptides.

For comparison purposes, the MD simulation of the ligand-free enzyme and 2 MD simulations of cis and trans forms of unbound substrate were performed in a water sphere (r = 25 Å). The 1RMH crystal structure was used for the ligand-free enzyme simulation and Suc-AGPF-*p*NA was used for free substrate simulations. These simulations followed the same procedure as detailed in the CyP•ligand complex simulations.

The contact area between the ligand and the enzyme was calculated, using the program NACCESS, from the coordinates of CyP•ligand averaged over each 100 ps of production dynamics.[28] Standard atomic radii and a slice thickness of 0.05 Å were used for the calculation.

(14) Fischer, S.; Michnick, S.; Karplus, M. *Biochemistry* **1993**, *32*, 13830−13837.
(15) Orozco, M.; Tirado-Rives, J.; Jorgensen, W. L. *Biochemistry* **1993**, *32*, 12864−12874.
(16) Harrison, R. K.; Stein, R. L. *J. Am. Chem. Soc.* **1992**, *114*, 3464−3471.
(17) Sierkierka, J. J.; Hung, S. H. Y.; Poe, M.; Lin, C.; Sigal, N. H. *Nature* **1989**, *341*, 755−757.
(18) Harding, M. W.; Galat, A.; Uehling, D. E.; Schreiber, S. L. *Nature* **1989**, *341*, 758−760.
(19) MacKerell, J., A. D.; Bashford, D.; Bellott, M.; Dunbrack, R. L., Jr.; Evanseck, J. D.; Field, M. J.; Fischer, S.; Gao, J.; Guo, H.; Ha, S., Joseph-McCarthy, D.; Kuchnir, L.; Kuczera, K.; Lau, F. T. K.; Mattos, C.; Michnick, S.; Ngo, T.; Nguyen, D. T.; Prodhom, B.; Reiher, W. E., III; Roux, B.; Schlenkrich, M.; Smith, J. C.; Stote, R.; Straub, J.; Watanabe, M.; Wiorkiewicz-Kuczera, J.; Yin, D.; Karplus, M. *J. Phys. Chem. B* **1998**, *102*, 3586−3616.
(20) Kern, D.; Kern, G.; Scherer, G.; Fischer, G.; Drakenberg, T. *Biochemistry* **1995**, *34*, 13594−13602.
(21) Wiberg, K. B. *Acc. Chem. Res.* **1999**, *32*, 922−929.
(22) Zhao, Y.; Ke, H. *Biochemistry* **1996**, *35*, 7356−7361.
(23) Vajdos, F. F.; Yoo, S.; Houseweart, M.; Sundquist, W. I.; Hill, C. P. *Protein Sci.* **1997**, *6*, 2297−2307.
(24) Brooks, B. R.; Bruccoleri, R. E.; Olafson, B. D.; States, D. J.; Swaminathan, S.; Karplus, M. *J. Comput. Chem.* **1983**, *4*, 187−217.
(25) Jorgensen, W. L.; Chandrasekhar, J.; Madura, J. D.; Impey, R. W.; Klein, M. L. *J. Chem. Phys.* **1983**, *79*, 926−935.
(26) Brooks, C. L., III; Karplus, M. *J. Mol. Biol.* **1989**, *208*, 159−181.
(27) Brooks, C. L., III; Karplus, M. *J. Chem. Phys.* **1983**, *79*, 6312−6325.

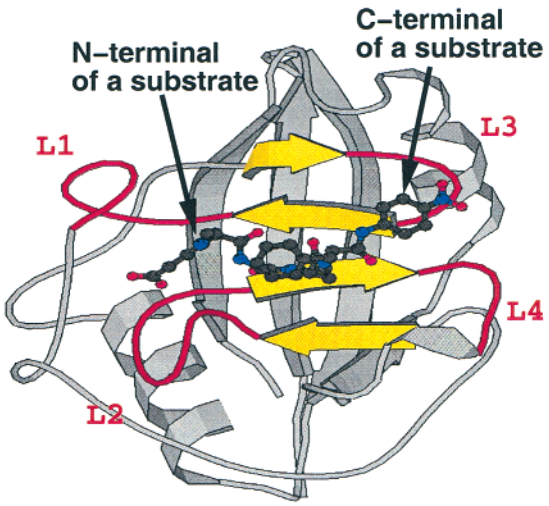

Figure 1. Ribbon structure of a cyclophilin (CyP) complexed with the substrate Suc-AGPF-*p*NA. The substrate binds to a channel formed by four loops (red coil L1, L2, L3, and L4). The nonreactive part (C-terminal and N-terminal part) of the substrate binds between those loops. The reactive part (X**C(=O)-N**Pro) of the substrate binds on the surface of the β-strands (yellow).

Results

The root-mean-squared deviation (RMSD) of the protein backbone α-carbons (CA) relative to the energy-minimized structure was used to select production dynamics intervals for the nine MD simulations of cyclophilin·ligand (ligand; Suc-AXPF-*p*NA: X = G, W, A, and L) and the MD simulation of ligand-free cyclophilin. All RMSD's of the 10 simulations reached equilibrium in 100−200 ps after the system was heated to 300 K. During the following 500 ps, the RMSD randomly fluctuates about values <2 Å with maximum RMSD remaining <2.5 Å. This portion of the dynamics was used for analysis in all ten simulations. For the simulations of *cis*- and *trans*-AGPF free in water, only the intervals where the substrate proline ring remained at the center of the sphere of water were chosen. This resulted in 400 ps of equilibrium state and was used for the following analysis.

Substrate Binding Site. The active site, formed by four β-sheets, resides on the surface of the enzyme (Figure 1). Four loops protrude out from the surface, forming a narrow channel where the substrate binds. The N-terminal part (Suc-Ala) of the substrate binds between the L1 and L2 loops and forms three hydrogen bonds with Gln63, Arg55, and Asn102. The C-terminal part (Phe-*p*NA) of the substrate binds between the other two loops (L3, L4), but the interaction between the enzyme and the ligand in this part is rather weak. The hydrophobic interaction between the aromatic ring of Trp121 and *p*NA of the substrate is the only one observed. The reactive part (X**C-(=O)-N**Pro) of the substrate binds between the N-terminal and C-terminal binding regions forming hydrophobic contacts with His126, Phe113, and Phe60 and electrostatic interaction with Arg55 and Asn102. When superimposing the averaged MD structure of the ligand-free CyP onto the CyP·*cis*, CyP·TS, and CyP·*trans* structures, the backbone matches well for all four structures with the exception of loop L2 being closer to L1 by ~1 Å before a ligand binds.

(28) Hubbard, S. J.; Thornton, J. M. NACCESS, Department of Biochemistry and Molecular Biology, University College: London, 1993.

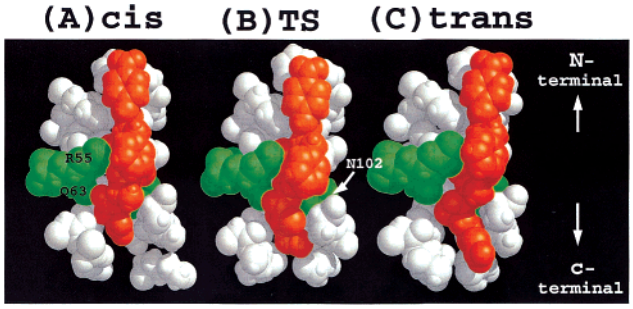

Figure 2. CPK view of CyP·*cis*-AAPF (A), CyP·TS-AAPF (B), and CyP·*trans*-AAPF (C). The orange molecule represents the AAPF and green residues are protein residues (Arg55, Gln63, and Asn102) which are in electrostatic interaction with the AAPF. The white residues are in van der Waals contacts with AAPF, but do not form hydrogen bonds with AAPF. It should be noted that same residues are shown in panels A, B, and C, although some residues contact only with one form of the ligand.

Table 1. Contact Area between CyP and Peptide

	AGPF		AWPF		AAPF			ALPF	
contact area (Å^2)	cis	TS	cis	TS	cis	TS	trans	cis	TS
hydrophobic	155	157	162	169	162	163	164	153	161
electrostatic	85	88	99	97	92	95	80	102	92
total	240	245	261	266	255	257	245	255	253

Contact Area between CyP and Cis-Isomer, TS, and Trans-Isomer. In the crystal structures of CyP·*cis*[22] and CyP·*trans*,[23] the position of the N-terminal region of the substrate differs compared to the similar positioning of the C-terminus. This suggests that the cis−trans isomerization is achieved by rotating the N-terminal rather than the C-terminal portion of the prolyl amide bond. The binding mode of *cis*-, *trans*-, and TS-AAPF to the CyP active site is depicted in Figure 2. The *trans*-AAPF is extended more than *cis*-AAPF by one residue and TS-AAPF has an intermediate extension. Despite the different positioning, calculation of the contact areas shows that CyP·*cis* and CyP·TS have similar electrostatic and hydrophobic contact areas, and the CyP·*trans* isomer is different only in the electrostatic interaction (Table 1). A closer examination of each interaction reveals that this similarity in the hydrophobic contact area of CyP·*cis*, CyP·TS, and CyP·*trans* results from the replacement of one interaction by another one when the N-terminal of the peptide turns. This is also the case for the electrostatic interaction of CyP·*cis* and CyP·TS. To compare the binding affinities more carefully, and to characterize catalytically important interactions, electrostatic interactions will be compared first between CyP·*cis* and CyP·TS, followed by comparison with CyP·*trans*. The three different electrostatic interaction modes are shown in Figure 3 and the detailed values are presented in Table. 2.

Electrostatic Interaction between CyP and Cis-Isomer or TS: 1. Pro. The positively charged Arg55 guanidino group is positioned right above the Pro(N) in both cis-isomer and TS (Figure 3A,B). The position of the guanidino group does not change during the dynamics (Figure 4A,B) and does not differ between CyP·*cis* and CyP·TS (Figure 4D). Despite no change in the position of the guanidino group, the interaction between Arg55 and the substrate Pro(N) becomes more favorable in CyP·TS than in CyP·*cis* due to the pyramidalization of the Pro(N); the Pro(N)···Arg55(NH2) distance is ~4.0 Å in CyP·*cis* and ~3.5 Å in Cyp·TS. The immobility of the guanidino group results from tight hydrogen bonding to the carbonyl Pro(O) in

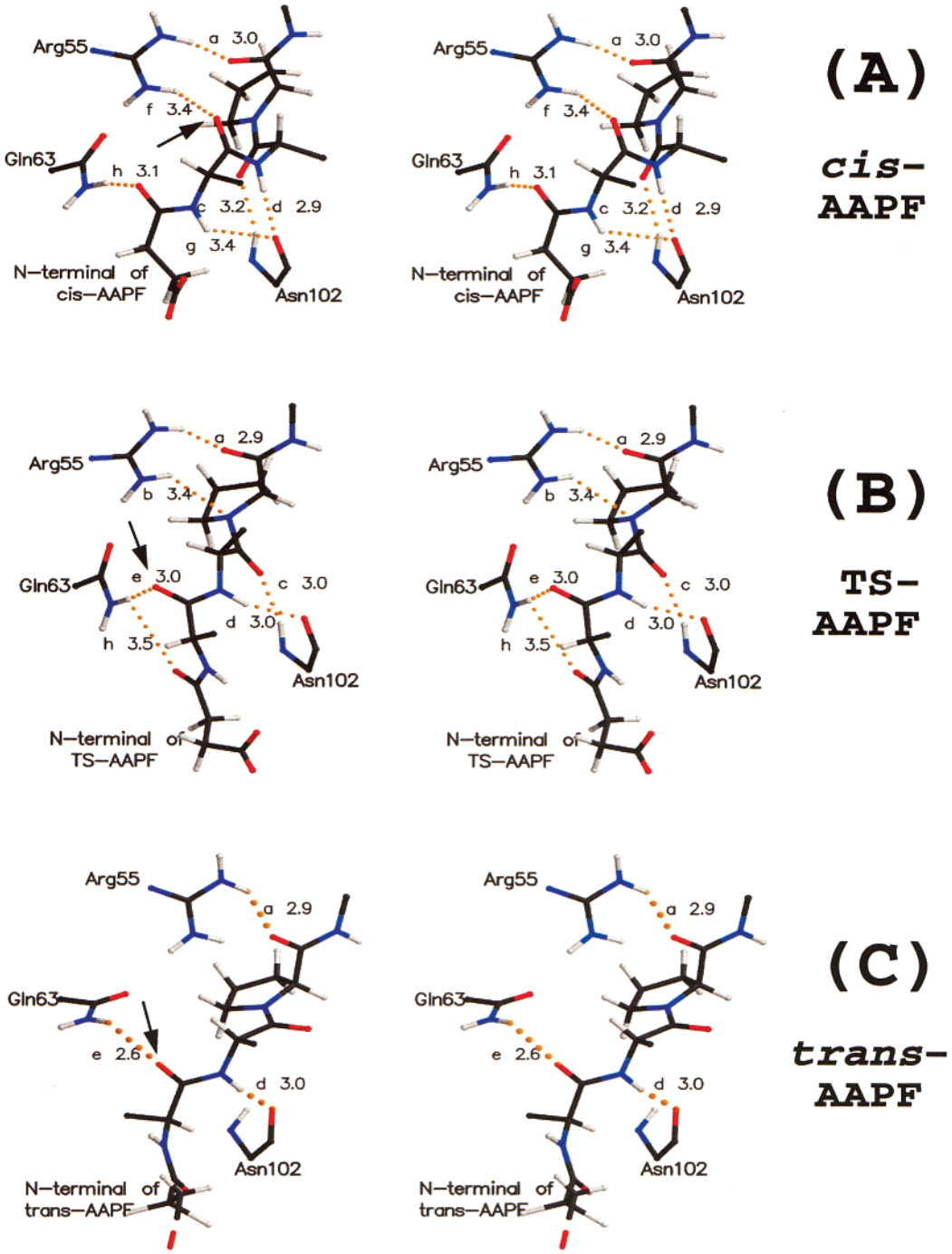

Figure 3. Stereoview of CyP·*cis*-AAPF (A), CyP·TS-AAPF (B), and CyP·*trans*-AAPF (C). The distances are between heavy atoms. Only interaction distances less than 3.5 Å are considered. The alphabet symbol identifies each interaction as designated in Table 2. To emphasize the turning of the N-terminal part of the peptide, the black arrow traces the movement of X(O) as the bond rotates from *cis*-AAPF through *trans*-AAPF.

both CyP·*cis* and CyP·TS (Figure 3A,B). As expected, without a ligand bound in the active site the guanidino group of Arg55 is highly disorganized (Figure 4C).

In addition to the Pro(O)···Arg55 interaction, there is another hydrogen bond Gln63(OE1)···Arg55 that holds the Arg55 guanidino group in the proximity of Pro(N) (Figure 4A,B). This interaction exists only in the presence of ligand. Without a ligand, Gln63 interacts with His54 rather than with Arg55 (Figure 4C), forming a different conformation of the Gln63 side chain (see Figure 4D). The conformational change of the Gln63 side chain upon substrate binding results in the interaction of Gln63 with the N-terminal part of the substrate. This conformation cannot be formed prior to ligand binding. Thus, substrate binding results in the change of the hydrogen bonding network in the CyP active site, from interaction between enzyme residues to interaction with the substrate. These altered hydrogen-bonding modes rigidly stabilize the newly formed geometrical arrangement that is preserved in CyP·TS.

2. X. When the amide carbonyl group X(C═O) is orthogonal to the proline ring in the CyP·TS, the X(O)···Asn102(HN) hydrogen bond length is shorter by 0.2−0.5 Å compared to that of the CyP·*cis* isomer (Figure 3A,B): 3.2 Å (CyP·*cis*-AAPF)

Table 2. Average Heavy Atom Distances (Å) of Electrostatic Interactions between the Ligand and the Enzyme Residues.

electrostatic interaction ligand···enzyme	letter symbol	AGPF		AWPF		AAPF			ALPF	
		cis	TS	cis	TS	cis	TS	trans	cis	TS
Pro(O)···Arg55(NH2)	**a**	2.91	2.87	2.86	2.91	2.98	2.92	2.86	2.96	2.89
Pro(N)···Arg55(NH1)	**b**	3.95	3.48	3.93	3.44	4.13	3.42	4.12	3.98	3.55
X(O)···Asn102(N)	**c**	3.66	3.12	3.22	3.01	3.18	2.98	6.14	3.27	5.40
X(N)···Asn102(O)	**d**	2.91	3.04	2.88	2.90	2.87	2.98	3.01	2.85	5.60
Ala(O)···Gln63(NE2)	**e**	5.35	4.15	5.27	2.90	5.73	3.01	2.86	5.41	3.11
Ala(O)···Arg55(NH1)	**f**	3.86	4.37	3.26	4.50	3.35	4.45	5.15	3.37	3.63
Ala(N)···Asn102(O)	**g**	3.33	3.30	3.24	3.57	3.41	3.89	4.97	3.23	6.08
Suc(O1)···Gln63(NE2)	**h**	3.07	3.49	3.09	3.62	3.07	3.45	7.39	3.09	4.27

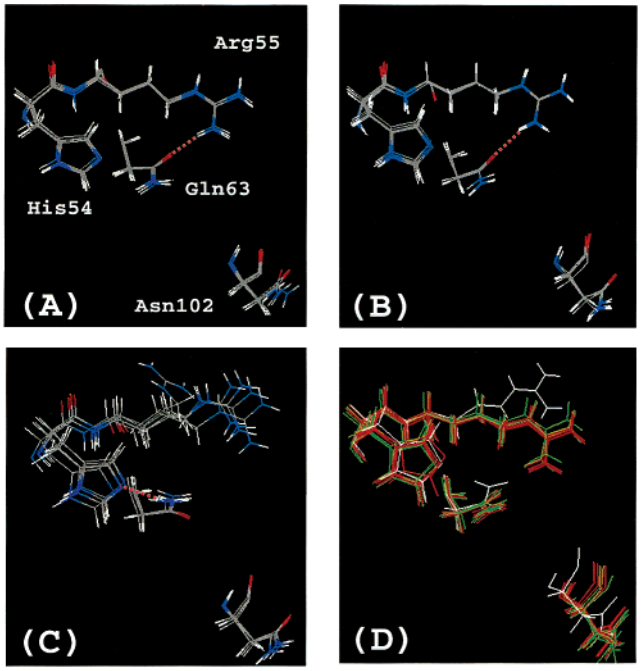

Figure 4. Superposition of the active site structures, each of which are averaged over 100 ps from the (A) CyP·*cis*-AAPF, (B) CyP·TS-AAPF, and (C) ligand-free CyP simulations. In panel D, the active site structures of 4 CyP·*cis*-AXPF (red), 4 CyP·TS-AXPF (green), and the ligand-free CyP (white) were compared, averaged over 500 ps of whole trajectories.

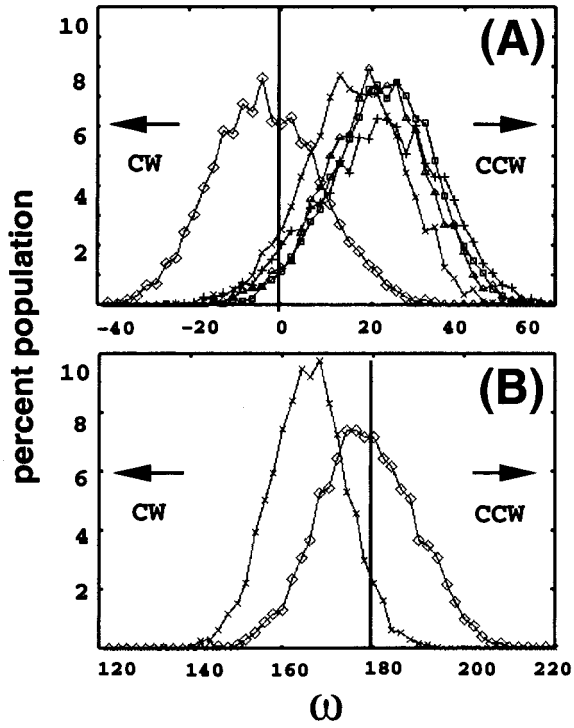

Figure 5. Population distribution of (A) cis- and (B) trans-isomer in the CyP active site and in water as a function of the amide bond distortion angle ω. AGPF (+), AWPF (□), AAPF (×), and ALPF(Δ) represent CyP-bound peptides and AGPF (◇) the free peptide in water. Arrows designate the direction in which the amide bond is distortedfrom the view of the *N*-terminal part of the peptide: clockwise (CW) or counterclockwise (CCW).

→ 3.0 Å(CyP·TS-AAPF). As in the interaction of Pro(N)··· Arg55, the shortening of this interaction distance from CyP·*cis* to CyP·TS results from the substrate conformational change rather than from the enzyme residue approaching the substrate. However, this more favorable hydrogen bond to the TS appears to be compensated by the ∼0.1 Å loosened hydrogen bond of X(HN)···Asn102(O) (Figure 3A and 3B): 2.9 Å (CyP·*cis*-AAPF) → 3.0 Å (CyP·TS-AAPF).

3. N-Terminal Part of the Peptide. Due to the little change in the position of Arg55, Gln63, and Asn102 during the reaction, a turning of the N-terminal part of the substrate caused by rotation of the X**C(═O)**−**N**Pro bond brings about a significant rearrangement of the interaction mode between enzyme and the N-terminus of the substrate (Figure 3A,B and Table 2). The hydrogen bond between Gln63(NE2) and Suc(O) present in CyP·*cis* is not present in CyP·TS. Instead, Gln63(NE2) forms a hydrogen bond with Ala(O) that is not hydrogen bonded in CyP·cis. The Ala(HN)···Asn102(O) and Ala(O)···Arg55(NH1) distances become longer by 0.2−0.4 and 0.3−1.0 Å, respectively, on going from CyP·*cis* to CyP·TS. Thus, the N-terminus of TS is not bound as tightly as that of cis-isomer.

Although this hydrogen bonding network rearrangement in the N-terminal region on conversion of CyP·*cis* → CyP·TS is observed in all four species of substrate, it should be noted that the extent of change depends on the identity of the X residue. Generally, the network rearrangement becomes more pronounced on going from X = Gly < Trp < Ala < Leu. The Suc(O)···Gln63(NE) distance change on CyP·*cis* → CyP·TS is smallest in X = Gly and largest in Leu. The formation of the hydrogen bond Ala(O)···Gln63(NE2) as CyP·*cis* → CyP·TS is not completed in the CyP· TS of X = Gly but fully accomplished in the CyP·TS of the other X's. The Ala(N)··· Asn102(O) interaction still exists in the TS of X = Gly but disappears as X changes to Trp > Ala > Leu.

Electrostatic Interaction between CyP and Trans-Isomer. The MD simulation of CyP·(*trans*-AAPF) shows similar positioning of Arg55, Asn102, and Gln63 as in CyP·*cis* and CyP·TS. In the CyP·*trans*-AAPF the guanidino group of Arg55 is held by Pro(O) and positioned above the Pro(N) as it is in CyP·*cis*-AAPF (Figure 3C). The hydrogen-bonding interaction between the amide X(HN) and Asn102(O) also remains in CyP·

trans, but the amide carbonyl X(O) in *trans*-AAPF is turned away from Asn102(HN) and does not form a hydrogen bond; X(O)···Asn102(N) distance = 6.14 Å. The hydrogen bonding network rearrangement in the substrate N-terminal region, on going from CyP·TS → CyP·*trans*-AAPF, is on the continuum of the rearrangement on CyP·*cis* → CyP·TS: Ala(O)···Gln63-(NE2) = 5.73 (cis) > 3.01 (TS) > 2.86 Å (trans), Ala(N)···Arg55(NH1) = 3.35 (cis) < 4.45 (TS) < 5.15 Å (trans), Ala(N)···Asn102(O) = 3.41 (cis) < 3.89 (TS) < 4.07 Å (trans), and Suc(O)···Gln63(NE2) = 3.07 (cis) < 3.45 (TS) < 7.39 Å (trans).

Conformational Change of Ground-State Peptides. Due to the hydrogen bond between Asn102(HN) and X(O) in CyP·*cis* (Figure 3A), the amide bond X**C(=O)−N**Pro is rotated counterclockwise by ∼20° from the cis-planar geometry (ω = 20 ± 14° for AGPF, 21 ± 11° for AWPF, 15 ± 11° for AAPF and 20 ± 11° for ALPF) (Figure 5A). For *trans*-AAPF, X(HN)···Asn102(O) interaction contributes to the distortion of the amide bond in the clockwise direction by 15° (ω = 165 ± 8°) (Figure 5B). These results are in clear contrast to the results from the simulations of peptide in water: ω is −4 ± 12° for *cis*-AGPF and 179 ± 11° for *trans*-AGPF (Figure 5). The distortion in the enzyme is achieved only in one direction (i.e. counterclockwise for cis-peptide and clockwise for trans-peptide), whereas in solution the amide bond fluctuates equally in both directions. However, it should be noticed that, even in water, there exist ground state conformers with the ∼20° twisted amide bond for both cis- and trans-isomers.

Chart 2

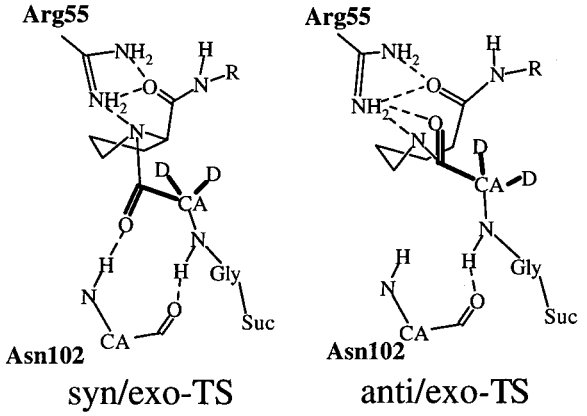

Complementarity of Anti/Exo-TS Structure to the Active Site. The correct geometry of TS in the active site is syn/exo-TS (Chart1). To assess the geometrical complimentarity of anti/exo-TS, an average structure of CyP·(syn/exo-TS-AGPF) was taken from the MD simulation of CyP·(TS-AGPF) and energy-minimized independently with a constraint of ω = −66° for CyP·anti/exo-TS and ω = 114° for CyP·syn/exo-TS. Comparison of these two energy-minimized structures shows only one significant difference in the interaction mode between the two TS structures and CyP. The Gly(O)···Asn102(HN) interaction in CyP·(syn/exo-TS) is replaced by Gly(O)···Arg55 in CyP·(anti/exo-TS), Gly(O)···Asn102(N) = 3.12 Å in CyP·(syn/exo-TS), and Gly(O)···Arg55(NH2) = 3.01 Å in CyP·(anti/exo-TS) (Chart 2). This difference in hydrogen bonding results in the dihedral angle θ (O−C−CA−HA1 or O−C−CA−HA2 of Gly of substrate) (depicted as a bold line in Chart 2) being ±60° in CyP·(syn/exo-TS) and 90°/180° in CyP·(anti/exo-TS).

Chart 3

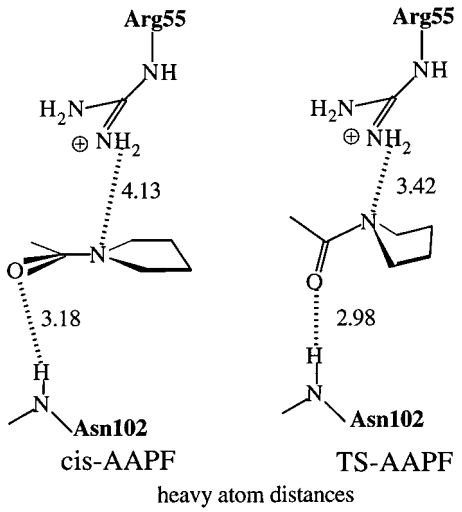

Discussion

Mechanism of Catalysis (Cis → Trans). The active site of the cyclophilin (CyP) consists of the domain surrounding the amide bond (X**C(=O)-N**Pro) of the substrate (Suc-Ala-X**C(=O)-N**Pro-Phe-*p*NA; X = Gly, Trp, Ala, and Leu) and the binding domains of the C-terminal and N-terminal parts of the substrate (Figure 1). The binding domain of the reactive part (X**C(=O)-N**Pro) undergoing the cis → trans reaction has two major catalytic features; the interaction of Asn102 with the amide carbonyl oxygen stabilizes the amide bond of the substrate with a 20° out-of-plane twist, while the position of the guanidino group of the Arg55 stabilizes localization of the lone pair developing at the amide Pro(N) during formation of the transition state (TS) (Chart 3). These two residues do not change in position when the cis-isomer is converted into the TS. This active site geometry is very stable (Figure 4A,B). The organization of the active site is supported by ligand−enzyme interaction and is accomplished on substrate binding (compare ligand-bound enzyme in Figure 4A/B with ligand-free enzyme in Figure 4C where Arg55 is highly disorganized and Asn102 is ∼1 Å off-positioned from the substrate-bound geometry). Comparison of these three structures, i.e., ligand-free and cis-bound and TS-bound CyP, shows that binding of the substrate to the active site provides all the geometrical organization necessary for the CyP reaction.

Although Asn102 and Arg55 are not repositioned in going from CyP·cis to CyP·TS, the more voluminous conformation of X**C(=O)-N**Pro of TS, compared to a planar geometry in cis-isomer, brings about a more intimate interaction of TS with CyP. The hydrogen bonding interaction of X(O)···Asn102(HN) is maximized when the carbonyl amide group is orthogonal to the proline ring in TS (Chart 3). Also, the interaction of Pro(N)···Arg55 is initiated on formation of CyP·TS due to the amide N pyramidalization (Chart 3).

1. Asn102. The X(O)···Asn102(HN) interaction is sufficient to stabilize the distortion of the amide bond of the cis-isomer by ∼20° counterclockwise. This distortion is efficiently performed because, while X(O) is attracted by Asn102(HN), the proline ring is held in position by a contact with the phenyl of

Chart 4

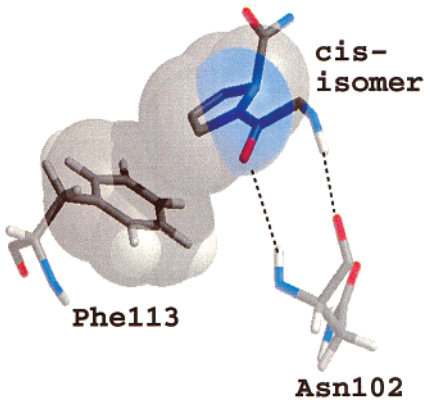

Phe113 (Chart 4). Computational studies have shown that the potential energy near the minimum is very flat and distortion up to 20° (corresponding to the ~10° out-of-plane angle in ref 21) increases the energy only by less than 0.5 kcal/mol. Indeed, our solution phase simulation of the *cis*-AGPF shows an existence of conformers with the ~20° distorted amide bond, formed by thermal fluctuations (Figure 5A). The ~20° distortion of the substrate amide bond found in the CyP·*cis* isomer can be interpreted as being due to CyP preferentially stabilizing the ~20° twisted conformer observed in solution.

This mechanism involving Asn102 is quite different than the "desolvation mechanism" proposed for the FKBP enzyme. In the desolvation mechanism, a hydrophobic environment surrounding the amide carbonyl O accelerates the amide bond rotation, supposedly by destabilizing the enolate-like resonance structure in GS.[29] This mechanism has been used to explain the ~2−3 kcal/mol decrease in the activation barrier when the reaction is transferred from water to nonpolar organic solvents[6] and to FKBP since this enzyme has a hydrophobic pocket surrounding the amide carbonyl.[14] However, recent computational studies provide grounds to question the significance of the enolate-like resonance contributor in the ground state of the amide by observing the following: the electron density at the carbonyl O decreases only by 0.04 electron unit and the bond length C═O is shortened no more than 0.01 Å as the amide bond rotates.[21] Although a specific hydrogen-bonding interaction between a water molecule and the amide carbonyl O has been shown to increase the rotation barrier by 2 kcal/mol compared to the gas-phase reaction,[6] Asn102 in CyP forms a hydrogen bond with the carbonyl O in the ground state at a distance 0.1−0.5 Å longer than in TS and thus preferential stabilization of GS compared to TS as in water is not expected in CyP.

2. Arg55. Arg55 is held in position by the interactions of Pro(O)···Arg55 (Figure 3) and of Gln63···Arg55 (Figure 4). In this geometry Arg55 does not interact with the amide Pro(N) in the ground state but is ready to interact with the lone pair in TS; the Pro(N)···Arg55 distance = ~4.0 Å (CyP·*cis*) → ~3.5 Å (CyP·TS). It often has been observed that orienting the potential hydrogen bond donor of the amide N, analogous to the Arg55 in the CyP reaction, in the ground state (GS) results in a conformer that closely resembles TS, contributing a rate enhancement in the cis−trans isomerization of the prolyl peptide. In the FKBP reaction, FKBP assists the formation of the intrasubstrate hydrogen bond of Pro(N)···Phe(HN) by restricting the GS conformation of enzyme-bound substrate (ψ = ~20°) in such a way that this interaction can be maximized at TS without changing the substrate turn structure ψ.[14] In aqueous solution, a disulfide bond in the peptide with the sequence -Cys-Pro-Phe-Cys- positions the Phe(HN) near the amide Pro(N) and the reaction rate is enhanced by ~10-fold compared to peptides without a disulfide bond.[30] These organizations in GS do not require an energetic destabilization of GS, but involve a geometrical arrangement of reactive components in a certain form (Near Attack Conformation, NAC) that directly leads to the corresponding TS without significant motion of these components.[3]

In a recent NMR study of the CyP·AFPF, a distinct profile of cross relaxation was observed in the backbone amide H of Arg55 as compared to other residues.[31] This result was interpreted as being due to a conformational change of the Arg55's backbone during the reaction cycle. Comparison of crystal structures of CyP·*cis*-Suc-AAPF-*p*NA (1RMH) and CyP·*trans*-HAGPIA (1AWQ) suggests that the backbone of Arg55 is similar for CyP·*cis* and CyP·*trans*. Our simulations of CyP·*cis*-AAPF, CyP·TS-AAPF, and CyP·*trans*-AAPF show no rearrangement in the backbone and side chain even in the TS. Considering that the amide backbone of Arg55 forms a strong antiparallel β-strand structure with the backbone of Gln63, a distinguishing motion only at the Arg55's backbone is less conceivable.

Comparison of Binding Modes between CyP·*cis* Isomer and CyP·TS. One of the prevalent explanations for enzymatic catalysis is that the TS is preferentially bound compared to the GS as determined by $K_m/K_{TS} = k_{cat}/k_{non}$ (Scheme 1).[2] To assess the validity of this position for the CyP reaction, we have compared the CyP binding mode of the cis form of the substrate and TS. The ratio of k_{cat}/k_{non} is 10^6 for CyP·*cis* → CyP·TS.[32] As was discussed above CyP residues (Asn102 and Arg55), which are residing at the reactive part (X**C(═O)-N**Pro) of the substrate, are organized to better fit the TS geometry (interaction **b** and **c** in Table 2 and Figure 3, see Chart 3). However, near the N-terminal part of the substrate four hydrogen bonds between the substrate and the enzyme are weaker in CyP·TS (interactions **d** and **f**−**h** in Table 2 and Figure 3) with only one hydrogen bond becoming stronger (interaction **e** in Table 2 and Figure 3). This is due to repositioning of the substrate's N-terminus relative to the protein when the X**C(═O)-N**Pro bond is rotated. The character of this rearrangement in the hydrogen-bonding network can be understood with better clarity when one considers the complete rearrangement on the conversion from the cis- through trans-isomer (see Figure 3 for stereoviews). In addition, comparison of hydrophobic contact areas in CyP·*cis* and CyP·TS shows that van der Waals interactions are similar in both CyP·*cis* and CyP·TS (Table 1). Thus, the contention that K_{TS} is a constant for E·TS dissociation and that $k_{cat}/k_{non} = K_m/K_{TS} = 10^6$ implies TS binds 10^6 more tightly than the ground state (GS) is not supported.

Mechanism of Catalysis (Trans → Cis). Our simulation of CyP·*trans*-AAPF is in accord with the catalytic role of Arg55

(29) Wolfenden, R.; Radzacki, A. *Chemtracts* **1991**, *2*, 52−54.
(30) Rabenstein, D. L.; Shi, T.; Spain, S. *J. Am. Chem. Soc.* **2000**, *122*, 2401−2402.
(31) Eisenmesser, E. Z.; Bosco, D. A.; Akke, M.; Kern, D. *Science* **2002**, *295*, 1520−1523.
(32) Kofron, J. L.; Kuzmic, P.; Kishore, V.; Colon-Bonilla, E.; Rich, D. H. *Biochemistry* **1991**, *30*, 6127−6134.

and Asn102 in the trans → cis reaction being the same as in cis → trans, i.e. stabilization of the localized lone pair at the amide N in TS by the guanidino group of Arg55 and distortion of the substrate amide bond by hydrogen bonding to the Asn102 backbone. Although in the cis → trans reaction the X(O)···Asn102(HN) hydrogen bond plays a major role in distorting the amide bond, this is replaced by the X(HN)···Asn102(O) interaction in the trans → cis reaction, resulting in 15° distortion of the amide bond clockwise from the view of the N-terminal part of the peptide. It is not difficult to imagine that X(O)···Asn102(HN) and X(HN)···Asn102(O) interactions observed in CyP·TS will be recovered by a 90° clockwise distortion of the amide bond of the trans-isomer and a 90° counterclockwise distortion of the amide bond of the cis-isomer. This satisfies the microscopic reversibility principle that forward and backward reactions have the same TS.

Selection of Syn/Exo-TS Structure in Preference to Anti/Exo-TS. When there is no direct chemical involvement by an enzyme in the reaction, examination of the "TS binding" tenet and the usefulness of K_{TS} becomes clearer because a direct path between the enzyme-bound TS and free TS in solution exists in the theoretical model of Scheme 1. According to this "TS binding" model, the geometrical complimentarity of the enzyme active site to the TS structure is the key feature of the enzyme activity and can be conversely used to determine the TS structure in the active site. At this point, it should be remembered that the prolyl peptide has four possible TS structures (Chart 1) in the water reaction[6,8] and we find both syn/exo- and anti/exo-TS configurations to fit almost equally into the active site when comparing the hydrogen-bonding interactions in the energy-minimized structure of CyP·(anti/exo-TS) and CyP·(syn/exo-TS) (see Results and Chart 2). However, secondary kinetic isotope effects (KIE)[13] suggest that anti/exo-TS does not occur in the active site as opposed to the reaction in water. The significantly larger k^H/k^D in the CyP reaction (1.13) compared to the water reaction (1.05) for Suc-Ala-Gly(D,D)-Pro-Phe-*p*NA implies that a specific geometrical conformation of bound TS enhances the hyperconjugation of Gly(D,D) compared to the free TS structure in water.[33] In a separate KIE study on carbonium ion solvolysis, the dependence of the extent of hyperconjugation on the dihedral angle (θ) between the C−D bond and the neighboring double bond has been experimentally measured by using geometrically constrained model molecules (k^H/k^D= 0.99 for $\theta = 0°/180°$, 1.01 for $\theta = 30°$, 1.07 for $\theta = 60°$, and 1.31 for $\theta = 90°$ for single β-deuterium substitution).[34] In our computational model, $\theta = \pm 30°$ in the syn/exo-TS and $\theta = 90°/180°$ in the anti/exo-TS. Applying these θ values to the experimentally determined relationship between θ and KIE,[34] the value of $k^H/k^D = 1.14$ is expected for the doubly deuterated syn/exo-TS and k^H/k^D= 1.30 for the doubly deuterated anti/exo-TS. To explain the experimental $k^H/k^D = 1.13$ in the CyP reaction, the TS in the active site is predominantly in syn/exo configuration even though, from our computational docking, anti/exo-TS is also compatible with the active site geometry.

Such a selection of the syn/exo-TS against the anti/exo-TS can be understood when one considers the geometry of the NAC.

(33) Previously, this enhanced KIE in CyP has been interpreted as being due to the enhanced hyperconjugation of β-deuterium in the hydrophobic environment of CyP. However, on going from water to organic solvent the KIE only increases by 1−2% and the active site of CyP is not even hydrophobic as is discussed.

(34) Shiner, V. J.; Humpherey, J. S. *J. Am. Chem. Soc.* **1963**, *85*, 2416−2419.

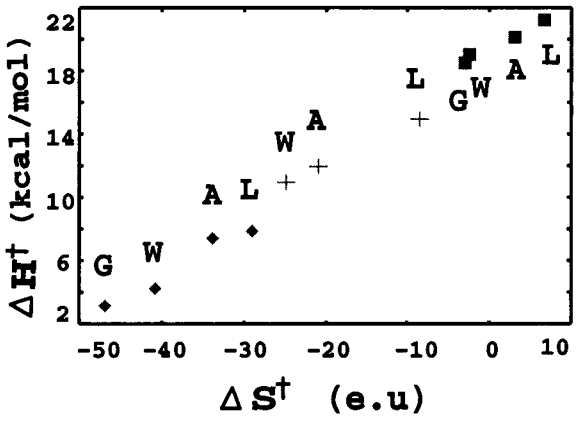

Figure 6. Entropy−enthalpy compensation phenomena measured in the CyP reaction (◆), FKBP reaction (+), and the noncatalyzed reaction in water (■). One-character symbols identify X residues of substrate Suc-AXPF-*p*NA. Data are taken from ref 13.

Asn102 distorts the amide bond counterclockwise for a cis-isomer, thereby the NAC resembles the syn-TS structure (Chart 2). Exo configuration of the TS structure is expected by the position of Arg55, which induces the development of the amide Pro(N) lone pair toward Arg55 (Chart 2). Thus, the TS structure in the active site is the one that is channeled through NACs and therefore the geometry of the NAC selects the TS structure.

The Rate Constants in Terms of the Mole Fraction of NACs. A NAC is defined as a conformer in which the amide carbonyl group is distorted by ≥20° from the planar geometry and the Pro(N)···Arg55(NH2) distance is smaller than 4.0 Å. These criteria were used for both cis → trans and trans → cis reactions catalyzed by CyP. In our simulation of CyP·*cis*-peptide, the carbonyl amide dihedral angle is turned counterclockwise on the average by 20° (CyP·AGPF), 21° (CyP·AWPF), 15° (CyP·AAPF), and 20° (CyP·ALPF) from the viewpoint of the N-terminus of the peptide (Figure 5A) and the guanidino group of Arg55 is organized at a distance from the Pro(N) at 3.95 (CyP·AGPF), 3.93 (CyP·AWPF), 4.13 (CyP·AAPF) and 3.98 Å (CyP·ALPF). These result in 34% (CyP·AGPF), 33% (CyP·AWPF), 12% (CyP·AAPF), and 28% (CyP·ALPF) of the ground state population existing as NACs. From these NAC populations, the variation of the activation barrier among these peptides is predicted to be less than 0.5 kcal/mol. This agrees with the experimentally determined k_{cat}/K_m within the error of 1 kcal/mol: 1200 (CyP·AGPF), 360 (CyP·AWPF), 3200 (CyP·AAPF), and 2700 $mM^{-1}s^{-1}$ (CyP·ALPF).[13] For CyP·*trans*-AAPF, the carbonyl amide dihedral is turned clockwise by 15° from the view of the N-terminal part of the substrate and the Arg55 to Pro(N) distance is 4.25 Å. When applying the same criteria of NAC, the population of NAC is 10% in CyP·*trans*-AAPF, which is similar to 12% in CyP·*cis*-AAPF. On the basis of these NAC populations, it can be predicted that the cis → trans and trans → cis reaction rates are comparable. Indeed, ^{1}H NMR line shape analysis suggested similar rate constants for both directions in the CyP reaction: 1015 s^{-1} for cis → trans and 1470 s^{-1} for trans → cis, with the substrate Suc-Ala-Phe-Pro-Phe-*p*NA.[20]

Entropy and Enthalpy Compensation. The little variation in $\Delta G^‡$ for the CyP reaction of cis → trans with the four tetrapeptides is known to be due to compensation between $\Delta H^‡$ and $T\Delta S^‡$ (Figure 6).[13] It is interesting that the like compensation

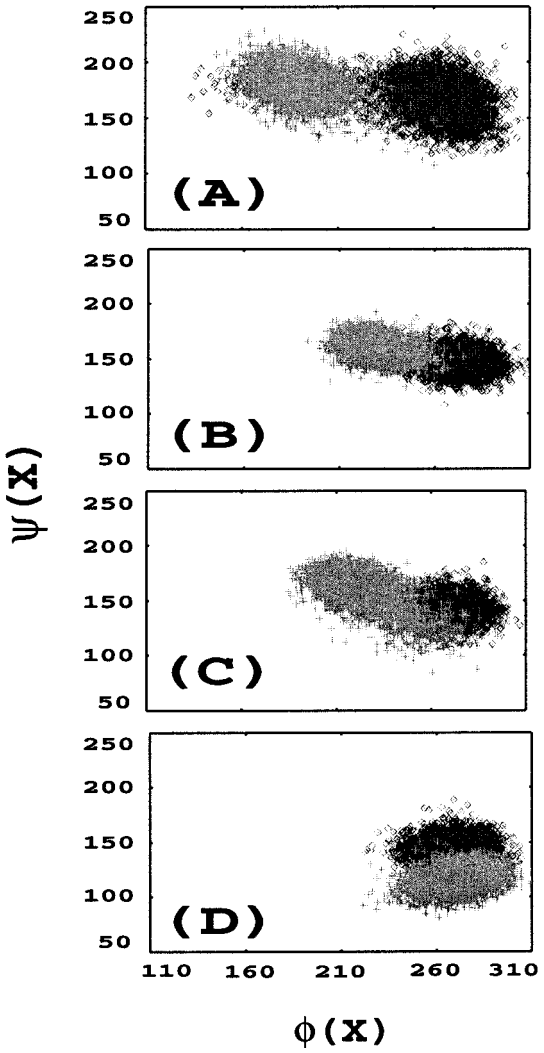

Figure 7. X residue conformational distribution as a function of ϕ(X) vs ψ(X) when X = Gly (A), Trp (B), Ala (C), and Leu (D) sampled in the CyP active site from the MD simulations. In each panel, black dots represent the cis-isomer and gray dots the TS.

of $\Delta H^{\ddagger}$ and $\Delta S^{\ddagger}$ is also observed for both the FKBP and water reactions. This phenomenon in the enzymatic reaction was initially explained in terms of the binding affinity of TS to the active site; i.e. tighter binding of TS (decrease in $\Delta H^{\ddagger}$) brings in a freezing the motion of TS (decrease in $\Delta S^{\ddagger}$).[13] This explanation would appear to be without merit considering that the same compensation of $\Delta H^{\ddagger}$ and $\Delta S^{\ddagger}$ is found with water solvent. Thus, the phenomenon is an attribute of the substrate not the enzyme. One may expect the effect originates from the X side chain directly affecting the X**C(=O)-N**Pro rotation and this effect is equally shifted when altering the environment. However, no direct interaction was observed between the X side chain and the X**C(=O)-N**Pro bond either in CyP·cis or in CyP·TS for all four tetrapeptides. We found in our simulation that a turning of the N-terminal part of the peptide in TS from the cis geometry becomes more pronounced in the same increasing order of experimentally obtained $\Delta S^{\ddagger}$. Figure 7 shows the distribution of cis and TS conformers over conformational space of ψ(X) vs ϕ(X). As X is mutated from Gly to Trp, to Ala, and to Leu the overlap between cis distribution and TS distribution becomes larger. Because ω(X**C(=O)-N**Pro) changes from 20° to 114° on the conversion of cis → TS for all four species, a large overlap between cis and TS over the conformational space of ψ(X) and ϕ(X) implies a large turn of the N-terminal part in TS. Indeed, the variation among the four TS peptides in their interaction mode between the N-terminal part and CyP (Table 2) confirms that the TS's N-terminus turns to a greater degree in the increasing order of X = Gly < Trp < Ala < Leu (see Results). It is not surprising to see the order of Gly < Ala < Leu because the larger size of the X side chain involves a higher tendency to preserve the intrinsically preferred internal conformation ψ and ϕ. The peculiarity of X = Trp, which turns less than Ala and Leu, despite having a bulkier side chain, can be explained in terms of a special conjunction with the substrate phenyl substituent. In the simulation of CyP·TS-AWPF the Trp ring is stacked with the substrate's phenyl ring and is stabilized in that conformation.

Such effect of the X residue on the N-terminal turning can be similarly expected in water as well as in FKBP and this independence of environment may explain the similar observation of the compensation phenomena in three different environments. Indeed, the larger conformational change between two equilibrium states in a "spectator" part of the whole system has been reported to bring in larger $\Delta S°$ and $\Delta H°$.[35] When applied to the GS and TS as two equilibrium states, the larger turning of the N-terminus of the peptide may explain the larger $\Delta S^{\ddagger}$ and $\Delta H^{\ddagger}$. The absence of compensation effect in the water reaction of dipeptide X**C(=O)-N**Pro also supports this proposition.[13]

Conclusion

Our molecular dynamics simulations of the ground state (GS) and the transition state (TS) for cyclophilin (CyP) catalysis of the cis−trans isomerization of prolyl peptides (Suc-Ala-X**C(=O)-N**Pro-Phe-*p*NA; X = Gly, Trp, Ala, and Leu) in aqueous solution have revealed the following features. Though planarity is favored in the prolyl peptide bond largely due to amide resonance stabilization, the thermal motions of the peptide bond at ambient temperature are about ±10° from planarity and can reach ±20° without significantly increasing the energy (<0.5 kcal/mol). CyP increases the population of these 20° distorted GS species by hydrogen bonding the amide carbonyl O to the Asn102 backbone amide group. Along with the formation of this 20° twisted ground state, the Arg55 guanidino group stabilizes development of the lone pair at the amide N in TS.

These two enzyme residues (i.e. Arg55 and Asn102) do not move in the course of CyP·*cis* → CyP·TS. However, this fixation is quite different in the ligand-free enzyme. Arg55 has considerable degrees of freedom and Asn102 is positioned differently in the enzyme free of substrate. Although Arg55 and Asn102 do not move during CyP·*cis* → CyP·TS, the interaction with Arg55 and Asn102 is preferentially favorable to the TS rather than to the cis-isomer due to the orthogonalization of the carbonyl group and pyramidalization of the amide N as cis → TS (Chart 3).

Despite the tighter binding of the X**C(=O)-N**Pro part of the TS compared to that of the cis-isomer, the TS as a whole is no more tightly bound than the cis-isomer. This is due to the less favorable interaction in the TS between protein and the N-terminus of the peptide, when N-terminus repositions while the C−N bond rotates. Examination of Figure 3 shows that, in

(35) Liu, L.; Guo, Q. *Chem. Rev.* **2001**, *101*, 673−695.

going from CyP·*cis*-AAPF to CyP·TS-AAPF, (i) interactions **b** and **e** appear, (ii) **c** becomes stronger, (iii) **d** and **h** become weaker, and (iv) **f** and **g** disappear when heavy atoms distances, less than 3.5 Å apart, only are considered (the letter symbol identifies interaction as designated in Table 2). Total hydrophobic interactions are also similar when comparing the hydrophobic contact areas of CyP·*cis* and CyP·TS. This is contradictory to the contention that the enzymatic catalysis is solely driven by the preferential binding of TS compared to GS by K_{TS}/K_m, which is 10^6 in the CyP reaction. Thus, K_{TS} in the thermodynamics cycle in Scheme 1 does not represent the dissociation constant of CyP·TS in water.

The organization of the reactive components on peptide binding creates a population of Near Attack Conformers (NACs) and this facilitates a reaction path toward a certain TS structure. This is because thermal motion of CyP·NAC can directly lead to the formation of the TS that most resembles the NAC. The syn configuration of the TS in Chart 1, which is formed by twisting the amide bond 90° counterclockwise from the view of the N-terminus of the peptide, is channeled through the ground-state conformer with the amide bond distorted ∼20° counterclockwise. The exo configuration of the TS is achieved by the position of Arg55, which is above the proline ring as compared to positioning below the ring (see Chart 2). The positioning of the Arg55 and the degree of distortion of the amide group of the bound substrate from the planar geometry are considered as criteria for Near Attack Conformers (NACs) in cis → trans rearrangement. NACs for the syn/exo-TS account for ∼30% of the total cis-ground-state population and other TS structures in Chart 1 are precluded from being formed, showing almost no occurrence of NACs toward these TS's. This is in good agreement with the experimentally determined KIEs, which also predict an exclusive occurrence of the syn/exo-TS. However, the geometry of the active site was seen to be almost equally complimentary to both the anti/exo- and the syn/exo-TS. This implies that the fitness of the TS cannot be a single determining factor for enzymatic reaction.

Acknowledgment. This study was supported by NSF grant MCB-9727937. We thank Dr. Kalju Kahn and Steve Szabo for helpful discussion. The authors gratefully acknowledge computer time on the University of California, Santa Barbara SGI Origin2000 and at the NPACI (San Diego Supercomputer Center).

JA020222S